



Synthesis, X-structure and solvent induced electronic states tuning of *meso*-tris(4-nitrophenyl)corrolato-copper complex

Dibyendu Bhattacharya, Pinky Singh, Sabyasachi Sarkar*

Department of Chemistry, Indian Institute of Technology-Kanpur, Kanpur 208 016, Uttar Pradesh, India

ARTICLE INFO

Article history:

Available online 15 July 2010

Dedicated to Prof. Achim Muller

Keywords:

Aerial oxidation
Copper(II)
Copper(III)
Corrole
Superoxide radical
X-ray

ABSTRACT

Copper(II) ion insertion into the coordination core of *meso*-tris(*p*-nitrophenyl)corrole (**1**), in air showed the formation of *meso*-tris(*p*-nitrophenyl)corrolatoCu(III) (**2**), with the generation of superoxide radical as the side product of the reaction. Single-crystal X-ray diffraction analysis revealed that **2** exhibits weak π - π stacking interaction. Among the two electronic states, diamagnetic Cu(III)-corrole³⁻ exists in DCM solution and in contrast is paramagnetic Cu(II)-corrole²⁻ cationic radical in DMF solution. This difference in electronic behavior in solution is due to the small energy gap between HOMO and LUMO that is readily influenced by solvent interaction.

© 2010 Elsevier B.V. All rights reserved.

1. Introduction

A large number of transition-metal complexes supported by a wide variety of non-innocent ligands (e.g. porphyrins, pterins, flavins, quinines, dithiolenes, or phenoxy based systems) have so far been evolved to evaluate the new aspects in synthetic chemistry and with special relevance to catalysis [1–5]. For macrocyclic, non-innocent corrole ligands, a great deal of efforts have been made to provide profound insights into the oxidation state of the metal centers [6–9]. High-valent metal ions have been reported to be present in copper, iron, chromium, cobalt, and manganese corroles [8]. It was thought that corrole ligand in these complexes has a non-innocent character, which has stimulated renewed interest in this field [6,10–12]. Corroles as free base are less stable than their porphyrin analogs in solution. Depending on the type and position of the substituents, corroles can readily transform to various products [13].

Copper is often used as the metal of choice for the synthesis and functionalization of metalocorroles, due to its easy insertion, the absence of an axial ligand and its diamagnetic ground state [14–18]. The Cu-metalation of corrole was first reported in 1965 [14]. Generally in basic medium and at room temperature several copper(II) compounds have been used for such metalation [19,20]. Cu-corroles are often oversimplified as Cu(III)-species with thermally accessible paramagnetic triplet excited state [15,16,21–25].

Furthermore, the electronic ground states of Cu *meso*-triarylcorroles (aryl = -C₆F₅, -CF₃, -OMe, -H, -CH₃) are sensitive to peripheral substituents and recently it has been reported that such Cu-corroles are inherently saddled as because of the Cu(d)-corrole(π) orbital interactions and thus electronic structure may be described as Cu(II)-corrole²⁻ cationic radical [26]. However, electronic nature of copper β -octaethylcorrole has been nicely scrutinized which indicates that ground state of the copper-corrole is best described as copper in 2+ physical oxidation state [27]. This was further verified with comparative DFT/XRD studies with analogs 10-oxacorrole copper(II) complex. The structure and electronic nature of the *meso*-tris(4-nitrophenyl)corrolato-copper complex has not yet been reported in the literature.

To understand the paradox of metal insertion inside the coordination core of corrole and its electronic structure in solution, we embarked on a study on the metalation of *meso*-tris(4-nitrophenyl)corrole and its related properties. Herein, we report on the mechanistic details of a simple synthetic methodology of a new *meso*-tris(4-nitrophenyl)corrolatoCu(III) corrole and also show the influence of a solvent to tune the relative ground state energy between the diamagnetic Cu(III)-corrole complex and paramagnetic, Cu(II)-corrole²⁻ cationic radical state.

2. Experimental

2.1. Materials and analytical methods

Solvents, pyrrole and aldehyde were obtained from S.D. Fine Chemicals Ltd., India and all solvents were dried and distilled

* Corresponding author. Tel.: +91 512 2597386; fax: +91 512 2597265.
E-mail address: abya@iitk.ac.in (S. Sarkar).

by standard methods prior to use [28]. *meso*-Tris(4-nitrophenyl)corrole (**1**) was prepared under condition developed by Paolesse et al. [29]. ^1H NMR spectrum of **1** and its microanalytical data were in good agreement with the reported data. Electronic absorption spectral measurements were recorded by USB 2000 (Ocean Optics Inc.) UV-Vis spectrophotometer equipped with fiber optics. X-ray diffraction data for **2** were collected on a Bruker-AXS smart APEX CCD diffractometer at 100 K. Infrared spectra were recorded on a Bruker Vertex 70, FT-IR spectrophotometer as pressed KBr disks. Elemental analyses for carbon, hydrogen and nitrogen were carried out with a Perkin-Elmer 2400 microanalyzer. Cyclic voltammetric measurements were performed with a BASi Epsilon-EC bioanalytical systems Inc. Cyclic voltammogram was recorded with glassy carbon electrode as working electrode, Pt wire as auxiliary electrode and Ag/AgCl electrode as reference electrode. All electrochemical experiments were done under argon atmosphere with 0.1 M Bu_4NClO_4 as supporting electrolyte at 298 K. Potentials are referenced against internal ferrocene (Fc) and are reported relative to the Ag/AgCl electrode ($E_{1/2}(\text{Fc}^+/\text{Fc}) = 0.49\text{ V}$ versus Ag/AgCl electrode). The scan rate of CV was 100 mV/s. Magnetic susceptibility was measured at 0.5 T as powder packed in gelatin capsules using a Quantum Design MPMSR2 SQUID susceptometer by heating the sample from 298 to 450 K. X-band EPR measurements were carried out on frozen solutions at 120 K on a Bruker EMX spectrometer. For the time dependent repetitive scan, the solution was thawed to bring it at room temperature in air and then cooled at 120 K to record the spectrum. EPR spectrometer setting: microwave frequency: 9.8 GHz, modulation amplitude: 10 G, modulation frequency: 100 kHz, microwave power: 0.21 mW.

Table 1
Summary of X-ray crystallographic data for **2**.

Compound	2
Empirical formula	$\text{C}_{37}\text{H}_{20}\text{Cu}_1\text{N}_7\text{O}_6$
Formula weight	722.15
T (K)	100 (2)
λ (Å)	0.71069
Crystal system	Monoclinic
Space group	$P2_1/c$
a (Å)	15.611(5)
b (Å)	16.462(5)
c (Å)	31.626(5)
α (°)	90
β (°)	109.493
γ (°)	90
V (Å ³)	7662(4)
Z	8
D_{calc} (mg cm ⁻³)	1.252
Crystal color, shape	Dark green, needle
Crystal size (mm)	$0.2 \times 0.1 \times 0.08$
$F(000)$	2944
Absorption coefficient (mm ⁻¹)	0.621
θ Range (°) for data collection	2.01–28.41
Index ranges	$-20 \leq h \leq 20$, $-22 \leq k \leq 17$, $-26 \leq l \leq 42$
Reflections collected	50 161
Unique reflections	18 984
Independent reflections (R_{int})	0.0992
Completeness to θ_{max} (%)	98.5
Data/restraints/parameters	18 984/0/836
Goodness-of-fit (GOF) on F^2	0.958
R_1^a , wR_2^b [$I > 2\sigma(I)$]	0.1019, 0.2359
R_1^a , wR_2^b (all data)	0.2421, 0.2516
Largest difference in peak and hole (e Å ⁻³)	0.84 and -0.93
Flack parameter	0.0

^a $R_1 = \sum ||F_o| - |F_c|| / \sum |F_o|$.

^b $wR_2 = \{ \sum [w(F_o^2 - F_c^2)^2] / \sum [w(F_o^2)^2] \}^{1/2}$.

2.2. Synthesis of *meso*-tris(4-nitrophenyl)corolato-copper(III) (**2**)

meso-Tris(*p*-nitrophenyl)corrole (**1**) (40 mg, 0.06 mmol) and $\text{Cu}(\text{acac})_2$ (0.48 mmol) were taken in 6 mL dichloromethane and triethylamine (0.20 mmol) was added into it. Color of the solution was finally changed from green to red-brown. The solution was further stirred at room temperature for 15 min in the presence of air and finally vacuum dried. The residue was then dissolved in dichloromethane and it was subjected to flash column chromatography using silica gel (100–200 mesh) and the eluted was evaporated under reduced pressure. Single crystal suitable for X-ray analysis of this compound was grown in a 1:1 mixture of dichloromethane and hexane. Yield = 45 mg, 80%. *Anal.* Calc. for $\text{C}_{56}\text{H}_{92}\text{N}_6\text{Cu}(\text{III})$: C, 73.69; H, 10.15; N, 9.20. Found: C, 73.39; H, 10.55; N, 9.41%. *Vis.* $\lambda_{\text{max}}/\nu_{\text{nm}}$ ($\epsilon/\text{M}^{-1}\text{cm}^{-1}$) in DCM: 424 (2.6×10^4), 553 (1.8×10^4), 660 (8.5×10^4).

2.3. Crystal structure determination of **2**

Crystals of **2** suitable for a diffraction study were prepared by slow diffusion of hexane into their dichloromethane solutions, mounted on glass fiber and transferred to a Bruker Smart CCD diffractometer. Details of the structure determinations are given in Table 1. Measurement was performed using graphite-monochromatized Mo $K\alpha$ radiation ($\lambda = 0.71073\text{ Å}$). The unit cell parameters and crystal-orientation matrices were determined by least-squares refinements of all reflections. The intensity data were corrected for Lorentz and polarization effects and an empirical absorption correction were also employed using the SAINT program [30]. Data were collected by applying the condition $I > 2\sigma(I)$. Intensity data were collected at 100(2) K within the limits $0.95^\circ < \theta < 28.30^\circ$ for **2**. The structure was solved by direct methods and followed by successive Fourier and difference Fourier syntheses. Full-matrix least-squares refinements on F^2 were carried out using SHELXL97 with anisotropic displacement parameters for all non-hydrogen atoms. Hydrogen atoms were constrained to ride on the respective carbon or nitrogen atoms with isotropic displacement parameters equal to 1.2 times the equivalent isotropic displacement of their

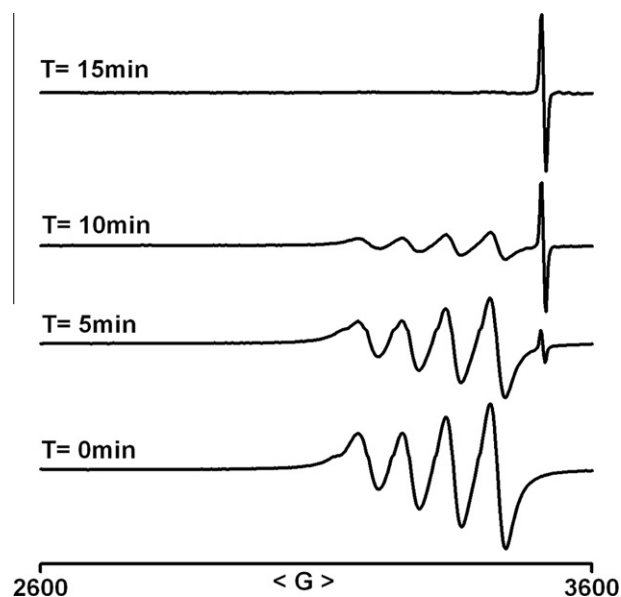
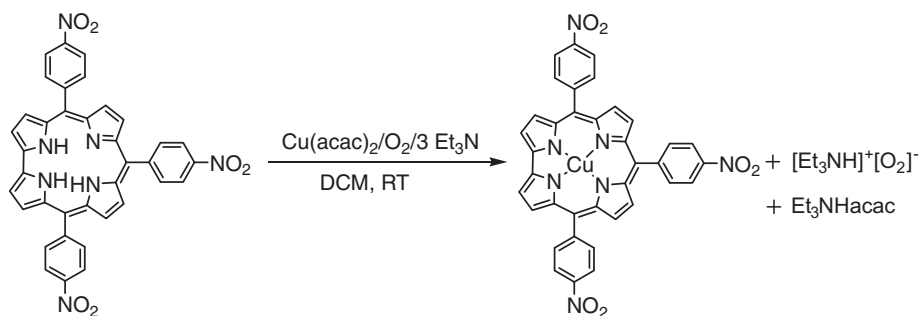


Fig. 1. Time dependent changes in the EPR spectral line shape (X-band, 120 K) monitored in dichloromethane with 1% triethylamine containing a mixture of $\text{Cu}(\text{acac})_2$ and corrole **1** (1:1) in air.



Scheme 1. Reaction involved in the course of copper insertion inside the corrole moiety.

parent atom in the all cases. Complex neutral atom scattering factors were used throughout for all cases. All calculations were carried out using SHELXS97 [31], SHELXL97 [32], PLATON99 [33], and ORTEP-3 [34] programs. The figures are generated by using the DIAMOND 3.1e program.

The structure of **2** suffered from disordered and unidentified solvent (crystallized from DCM–Hexane) in the lattice, which was not included in the refinement but was taken care of by the SQUEEZE procedure (from PLATON). The volume occupied by the solvent was 1079.5 Å³ and the number of electrons per unit cell deduced by SQUEEZE was 65.5.

3. Computational details

All calculations were performed with the GAUSSIAN 03, revision B.04, package [35]. Molecular orbitals were visualized using “Gauss View 3.0”. Gas-phase and single-point calculation was performed based on density functional theory (DFT). The method used was Becke’s three-parameter, hybrid exchange functional [36,37], the non-local correlation was provided by the Lee, Yang, and Parr expression (B3LYP), and by the Vosko, Wilk, and Nusair (1980) correlation functional (III) for local (B3LYP). The 6-31g(d,p) basis set [38] was used for H, C, and N atoms; the LANL2DZ [39] basis set and LANL2 pseudopotentials of Hay and Wadt [40] were used for Cu atoms. The geometry of **2** was obtained from its crystal structure.

4. Results and discussion

4.1. Synthesis of copper complex (2)

To understand the metalation of corrole, the synthesis of [*meso*-tris(*p*-nitrophenyl)corrolato]copper(III) (**2**) was carried out by the reaction of Cu(acac)₂ with the *meso*-tris(*p*-nitrophenyl)corrole [T(*p*-NO₂-P)Corr] (**1**) in dichloromethane in the presence of a few drops of triethylamine used as proton abstractor instead of carrying out the reaction in neat pyridine [14]. The metal insertion inside the coordination core of **1** was followed by monitoring the progress of the reaction by EPR spectroscopy (Fig. 1).

The diminution of the EPR signal of Cu(II) in Cu(acac)₂ concomitant with the appearance of EPR signal due to O₂⁻ radical [41] demonstrated the participation of the redox reaction between Cu(II) and aerial oxygen (Fig. 1). The dominant green color of **1** in the starting reaction mixture with Cu(acac)₂ changed to red-brown within minutes and 15 min was enough for the disappearance of the EPR signal arising from Cu(acac)₂. At the expense of this signal, a new EPR signal which started to appear within minutes became fully developed by this time. On standing for another 20 min, this signal disappeared. The identity of this EPR signal as O₂⁻ radical was revealed by the nitroblue tetrazolium assay [42,43] and the reaction that followed is shown in Scheme 1.

It is known in the metalation of corrole by copper(II) in air, that the isolated complex is found to be in copper(III) state [15–23].

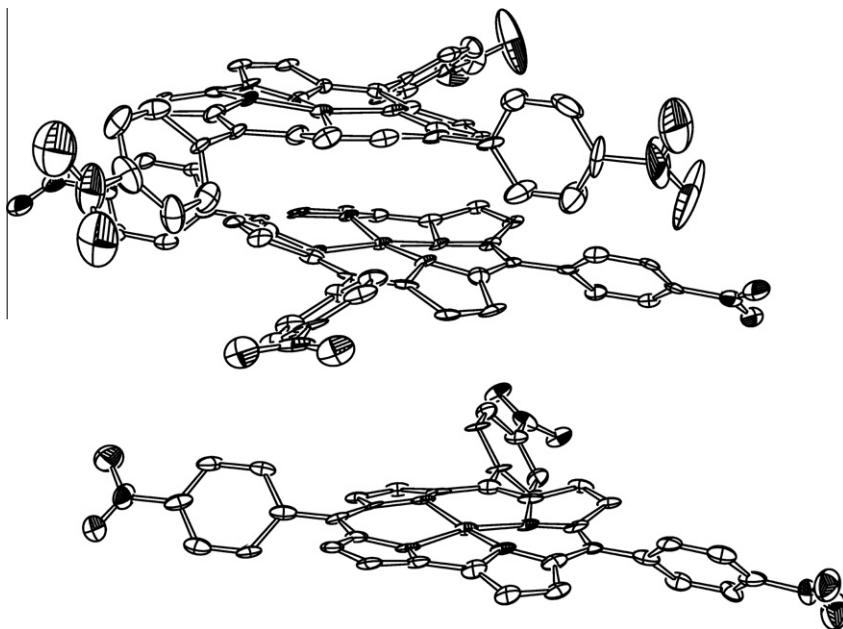


Fig. 2. Molecular structure of Cu[T(*p*-NO₂-P)C] (**2**). ORTEP representation with thermal ellipsoids at 50% probability (H atoms omitted for clarity).

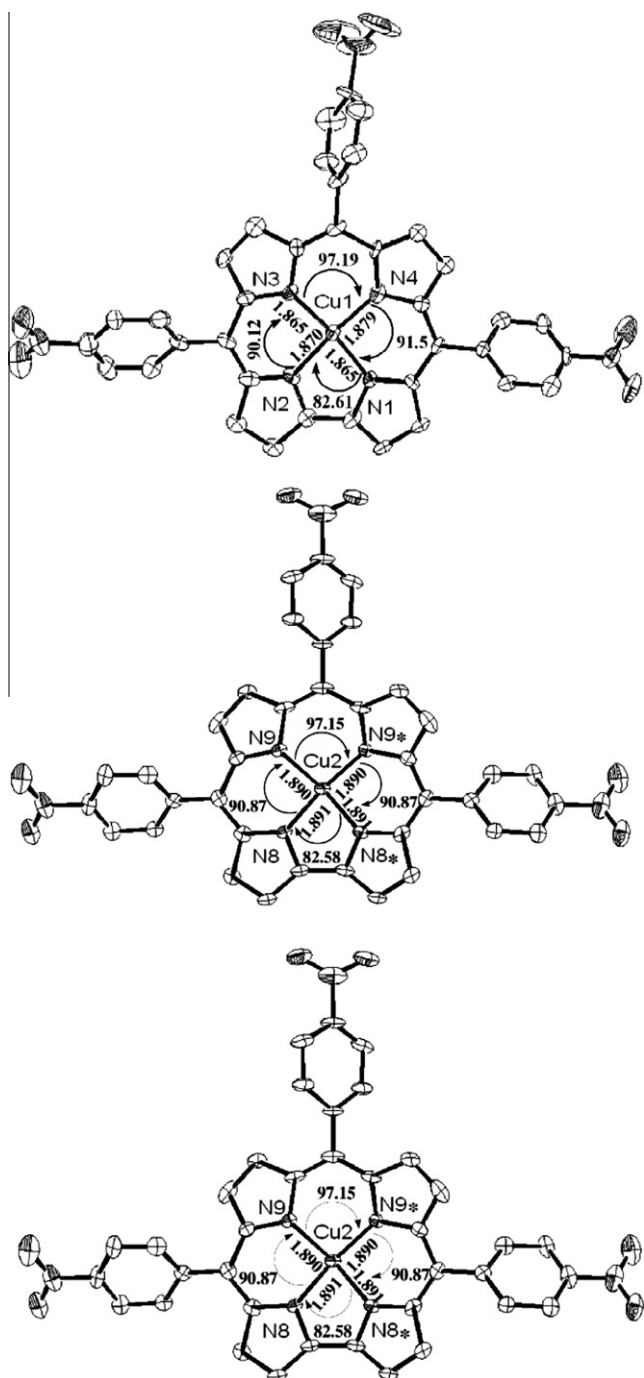


Fig. 3. Cu–N bond length and N–Cu–N angles of three molecules present inside the lattice of Cu(III)[T(p-NO₂-P)C] 2.

Though, the oxidizing agent in such reaction is aerial oxygen, its fate after the oxidation of Cu(II) to Cu(III) has not been identified. Thus the spontaneous generation of O₂^{•-} radical ion in the metalation of corroles by Cu(II) ion as a metal ion source is a rare event that is documented here.

4.2. Solid state structures of 2 by X-ray crystallography

ORTEP diagram of 2 are shown in Fig. 2 and the crystallographic data is provided in Table 1. Single-crystal X-ray structure analysis of 2 revealed that copper has been incorporated into the corrole core with no indication for the proton bound to the central nitrogen supporting the +3 oxidation state of the central metal atom.

The corrolato macrocycle form a saddle conformation with pyrrolic subunit tilted alternatively up and below the mean N₄ plane. The single crystal of 2 contains three crystallographically independent copper–corrole molecules with non-identical structural parameters (Fig. 3). As depicted in Fig. 2 these molecules interact with one another to form a π – π stacking. The intermolecular Cu–Cu distances between two successive planes in 2 are 4.478 Å and 4.113 Å, respectively, and mean distance between ring planes is 3.43 Å and 4.05 Å, respectively.

4.3. Electronic absorption spectroscopy

The electronic absorption spectra of the copper–corroles are exceptionally sensitive to peripheral substituents [13,17,18,26]. Substitution with electron-withdrawing group causes red-shifted optical spectra. Thus, Cu[T(p-H-P)C] shows absorption at 413 nm, but Cu[(CF₃)₈T(p-XP)C] complex shows absorption at 462 nm in DCM [7]. Compound 2 shows Soret band at 424 nm in DCM which is consistent with the expected red-shift compared to Cu[T(p-H-P)C] and blue-shift compared to Cu[(CF₃)₈T(p-XP)C]. Interestingly, 2 in DMF solution shows different electronic spectrum. Although Soret band appeared at the same position that found in DCM but there is a new peak at 649 nm appeared in DMF. This is probably due to the different electronic states in two different solvents. In DCM, compound 2 exists as a Cu(III)–corrole³⁻, however in DMF it exists as Cu(II)–corrole²⁻. This is further confirmed by the solution magnetic moment measurement, EPR, cyclic voltammetry and DFT studies as discussed below. Compound 2 displayed a broad absorption around 850 nm in DCM and also in DMF with subtle variation (Fig. 4). The origin of this broad absorption which is reproducible is not clear and requires further study.

4.4. Electron spin resonance and solution magnetic moment

Compound 2 is EPR inactive in the solid state and diamagnetic in the temperature range from 273 K to 450 K, suggesting its d⁸ electronic configuration in a square planar Cu(III) form [6,16,25]. In dichloromethane solution, it does not show any EPR signal. However, in DMF medium, it showed a broad EPR signal that may be related to Cu(II) state along with a free radical signal (g = 2.003). The narrow line width without any hyperfine structure

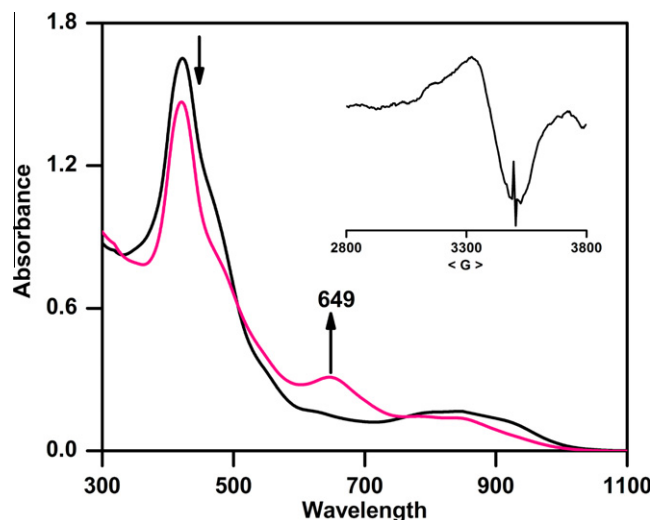


Fig. 4. Comparison of electronic spectra of 2. 2×10^{-4} (M) dichloromethane solution (black), DMF solution (pink). Inset indicates the EPR spectra of 2 in DMF solution, flat cell, RT. (For interpretation of the references in color in this figure legend, the reader is referred to the web version of this article.)

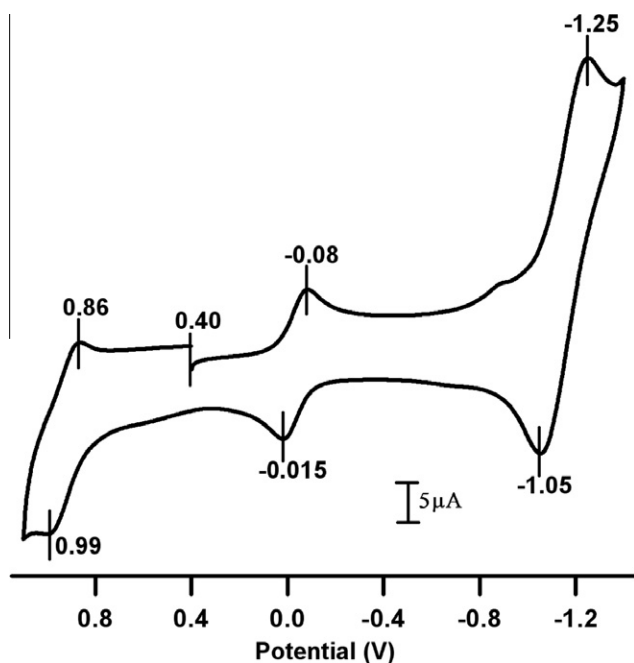


Fig. 5. Cyclic voltammogram of **2** in DCM (1 mM) in 0.1 M TBAPF₆ with scan rate, 100 mV/s vs. Ag/AgCl.

of the free radical signal indicated its identity as carbon centered radical (Fig. 4, inset). In DMF solution, the magnetic moment value

of **2** measured by Evans method showed $\mu_{\text{eff}} = 2.4$ BM, a value intermediate between one and two unpaired electrons (see Supplementary material).

4.5. Electrochemistry

The cyclic voltammetric (CV) trace of the Cu^{III}/Cu^{II} couple of **2** showed reversible value at $E_{1/2} = -0.04$ V (Fig. 5). Reversibility of this low potential $E_{1/2}$ was checked by the anodic peak I_{p_a} versus $v^{1/2}$ plot indicating the (scan rate 100–1000 mV/s) linear nature. The separation between anodic and cathodic peak current is close to one of the peak-to-peak separation observed for Fc/Fc⁺ couple in the same condition further substantiating the process as an one electron redox event. As corrole macrocycle is ‘non-innocent’ in nature that was reflected from the oxidation of the ring at a potential $E_{1/2} = +0.92$ V and two electron reversible reduction of –NO₂ group present periphery of the ligand in **2**.

Further inside into the metal center redox potential was obtained by comparing the potential with other reported copper–corrole as shown in Table S1 in Supplementary material.

Reduction potential of our system was found to be more positive in comparison to the other system which reflects the effect of the electron-withdrawing effect of the –NO₂ group. Thus the redox potential of the pentafluorophenyl corrole is –0.51 V but for –NO₂ substituted corrole such value appeared at –0.045 V. So, *meso* substituents in metalocorroles exert a strong influence on the half wave potential for one electron metal center reduction and this potential is shifted from –0.55 V to –0.045 V, when the *meso* substituents vary from *p*-OCH₃ phenyl to *p*-NO₂ phenyl group [17]. Thus,

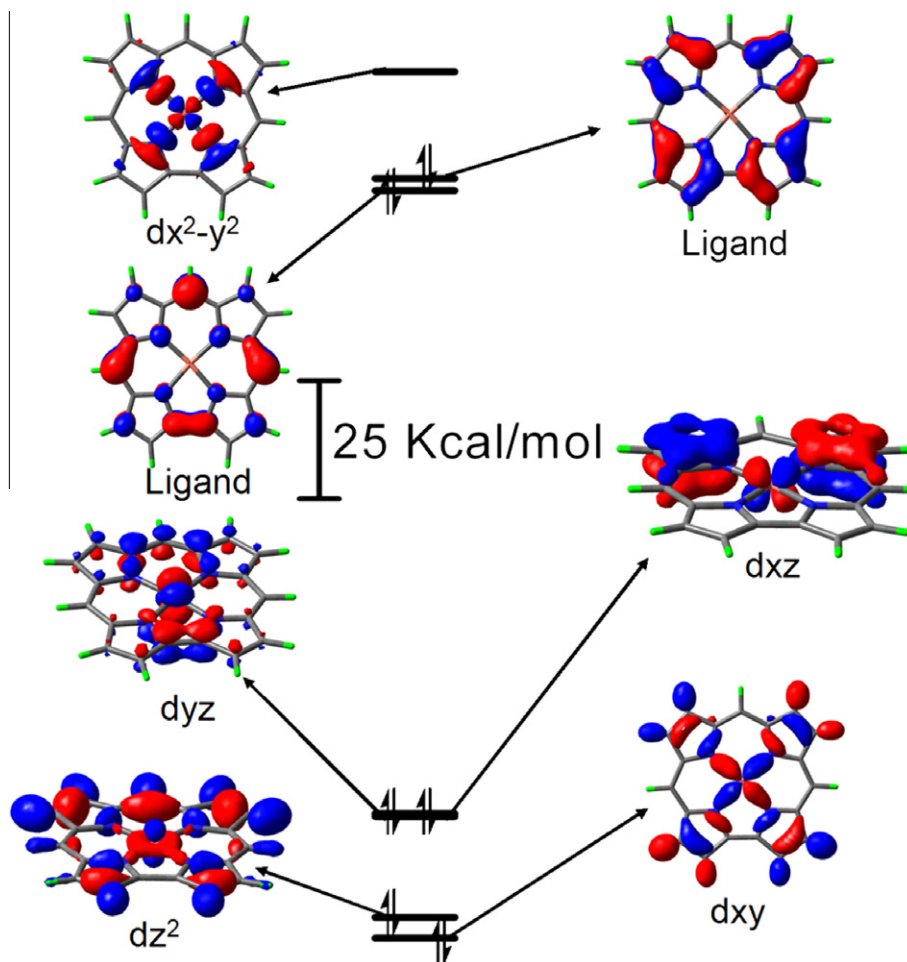


Fig. 6. Frontier molecular orbitals determined at the DFT B3LYP/LanL2DZ level for unsubstituted Cu(III)-corrole.

it is easier for the $[(p\text{-NO}_2\text{-P})\text{C}]\text{Cu}^{\text{III}}$ to be reduced compared to that of $[(p\text{-OCH}_3\text{-P})\text{C}]\text{Cu}^{\text{III}}$ analogs.

4.6. DFT calculations

Geometry optimized ground state MO's were performed on the unsubstituted copper–corrole by DFT method. The HOMO and HOMO-1 are ligand based and LUMO is metal based with $d_{x^2-y^2}$. The energy difference between LUMO and HOMO is only 27 kcal/mol (Fig. 6) and such a small energy gap may be easily manipulated by the solvation energy provided by the solvent. Thus, although +3 oxidation state of Cu is stable in nonpolar solvent, intramolecular electron transfer facilitated by polar medium (by favorable mixing of the d-orbitals of metal ion with the orbital of the corrole ring) made Cu(II)–corrole²⁻ state to be stable in the polar solvent. [44–48].

5. Conclusions

The chemistry associated with Cu metal insertion inside the coordination core of corrole has been successfully investigated to show that the air present in the reaction mixture oxidized the Cu(II) ion to Cu(III) with the generation of O₂⁻. The X-ray structure of this new copper–corrole showed saddle conformation with three crystallographically independent copper–corrole molecules interacting through weak π – π stacking with non-identical structural parameters. Solvent induced changes in the electronic states were confirmed by UV–Vis, EPR, solution magnetic moment and cyclic voltammetric measurements. This difference in electronic behavior in different solvents is due to the small energy gap between LUMO and HOMO. The propensity of other first row transition–metal–corrole complexes with different solvent is under investigation.

Acknowledgements

D.B. acknowledges IIT Kanpur for a Senior Teaching Fellowship, P.S. for a Senior Research Fellowship from the CSIR, New Delhi and S.S. thanks the DST, New Delhi for funding the project.

Appendix A. Supplementary material

CCDC 771021 contains the supplementary crystallographic data for this paper. These data can be obtained free of charge from The Cambridge Crystallographic Data Centre via www.ccdc.cam.ac.uk/data_request/cif. Supplementary data associated with this article can be found, in the online version, at [doi:10.1016/j.ica.2010.07.016](https://doi.org/10.1016/j.ica.2010.07.016).

References

- [1] A. Mohammed, Z. Gross, *J. Am. Chem. Soc.* 127 (2005) 2883.
- [2] M.R. Ringenberg, S.L. Kokatam, Z.M. Heiden, T.B. Rauchfuss, *J. Am. Chem. Soc.* 130 (2008) 788.
- [3] M.W. Bouwkamp, A.C. Bowman, E. Lobkovsky, P.J. Chirik, *J. Am. Chem. Soc.* 128 (2006) 13340.
- [4] C. Stanciu, M.E. Jones, P.E. Fanwick, M.M. Abu-Omar, *J. Am. Chem. Soc.* 129 (2007) 12400.
- [5] M.R. Haneline, A.F. Heyduk, *J. Am. Chem. Soc.* 128 (2006) 8410.
- [6] I. Luobeznova, L. Simkhovich, I. Goldberg, Z. Gross, *Eur. J. Inorg. Chem.* (2004) 1724.
- [7] E. Steene, A. Dey, A. Ghosh, *J. Am. Chem. Soc.* 125 (2003) 16300.
- [8] Z. Gross, *J. Biol. Inorg. Chem.* 6 (2001) 733.
- [9] L. Simkhovich, A. Mahammed, I. Goldberg, Z. Gross, *Chem. Eur. J.* 7 (2001) 1041.
- [10] S. Cai, F.A. Walker, S. Licoccia, *Inorg. Chem.* 39 (2000) 3466.
- [11] O. Zakharieva, V. Schünemann, M. Gerdan, S. Licoccia, S. Cai, F.A. Walker, A.X. Trautwein, *J. Am. Chem. Soc.* 124 (2002) 6636.
- [12] S. Nardis, R. Paolesse, S. Licoccia, F.R. Fronczek, M.G.H. Vicente, T.K. Shokhireva, S. Cai, F.A. Walker, *Inorg. Chem.* 44 (2005) 7030.
- [13] C.P. Gros, J.-M. Barbe, E. Espinosa, R. Guillard, *Angew. Chem., Int. Ed.* 45 (2006) 5642.
- [14] A.W. Johnson, I.T. Kay, *J. Chem. Soc.* (1965) 1620.
- [15] M. Stefanelli, M. Mastroianni, S. Nardis, S. Licoccia, F.R. Fronczek, K.M. Smith, W. Zhu, Z. Ou, K.M. Kadish, R. Paolesse, *Inorg. Chem.* 46 (2007) 10791.
- [16] S. Will, J. Lex, E. Vogel, H. Schmickler, J.-P. Gisselbrecht, C. Hauptmann, M. Bernard, M. Gross, *Angew. Chem., Int. Ed.* 36 (1997) 357.
- [17] I.H. Wasbotten, T. Wondimagegn, A. Ghosh, *J. Am. Chem. Soc.* 124 (2002) 8104.
- [18] A. Ghosh, T. Wondimagegn, A.B.J. Parusel, *J. Am. Chem. Soc.* 122 (2000) 5100.
- [19] C.V. Asokan, S. Smeets, W. Dehaen, *Tetrahedron Lett.* 42 (2001) 4483.
- [20] W. Maes, T.H. Ngo, J. Vanderhaeghen, W. Dehaen, *Org. Lett.* 9 (2007) 3165.
- [21] C. Bruckner, R.P. Brinas, J.A. Krause Bauer, *Inorg. Chem.* 42 (2003) 4495.
- [22] D.T. Gryko, M. Tasiar, T. Peterle, M. Bröring, *J. Porphyrins Phthalocyanines* 10 (2006) 1360.
- [23] Y. Gao, J. Liu, M. Wang, Y. Na, B. Åkermark, L. Sun, *Tetrahedron* 63 (2007) 1987.
- [24] Y. Gao, J. Liu, W. Jiang, M. Xia, W. Zhang, M. Li, B. Åkermark, L. Sun, *J. Porphyrins Phthalocyanines* 11 (2007) 463.
- [25] N. Maiti, J. Lee, S.J. Kwon, J. Kwak, Y. Do, D.G. Churchill, *Polyhedron* 25 (2006) 1519.
- [26] A.B. Alemayehu, E. Gonzalez, L.K. Hansen, A. Ghosh, *Inorg. Chem.* 48 (2009) 7794, and references cited therein.
- [27] M. Bröring, F. Brégier, E.C. Tejero, C. Hell, M.C. Holthausen, *Angew. Chem., Int. Ed.* 46 (2007) 445.
- [28] A.J. Vogel, *Practical Organic Chemistry*, fifth ed., Longmans, Prentice Hall, London, UK, 1964.
- [29] R. Paolesse, S. Nardis, F. Sagone, R.G. Khoury, *J. Org. Chem.* 66 (2001) 550.
- [30] Bruker–Nonius, APEX-II and SAINT-Plus, Bruker–AXS Inc., Madison, Wisconsin, USA, 2004.
- [31] G.M. Sceldrick, *SHELXS97*, Program for Solution of Crystal Structure, University of Göttingen, Göttingen, Germany, 1997.
- [32] G.M. Sceldrick, *SHELXL97*, Program for Crystal Structure Analysis (Release 97-2), University of Göttingen, Göttingen, Germany, 1997.
- [33] A.L. Spek, *J. Appl. Crystallogr.* 36 (2003) 7.
- [34] L.J. Farrugia, *J. Appl. Crystallogr.* 30 (1997) 565.
- [35] M.J. Frisch, G.W. Trucks, H.B. Schlegel, G.E. Scuseria, M.A. Robb, J.R. Cheeseman, J.A. Montgomery Jr., T. Vreven, K.N. Kudin, J.C. Burant, J.M. Millam, S.S. Iyengar, J. Tomasi, V. Barone, B. Mennucci, M. Cossi, G. Scalmani, N. Rega, G.A. Petersson, H. Nakatsuji, M. Hada, M. Ehara, K. Toyota, R. Fukuda, J. Hasegawa, M. Ishida, T. Nakajima, Y. Honda, O. Kitao, H. Nakai, M. Klene, X. Li, J.E. Knox, H.P. Hratchian, J.B. Cross, V. Bakken, C. Adamo, J. Jaramillo, R. Gomperts, R.E. Stratmann, O. Yazyev, A.J. Austin, R. Cammi, C. Pomelli, J.W. Ochterski, P.Y. Ayala, K. Morokuma, G.A. Voth, P. Salvador, J.J. Dannenberg, V.G. Zakrzewski, S. Dapprich, A.D. Daniels, M.C. Strain, O. Farkas, D.K. Malick, A.D. Rabuck, K. Raghavachari, J.B. Foresman, J.V. Ortiz, Q. Cui, A.G. Baboul, S. Clifford, J. Cioslowski, B.B. Stefanov, G. Liu, A. Liashenko, P. Piskorz, I. Komaromi, R.L. Martin, D.J. Fox, T. Keith, M.A. Al-Laham, C.Y. Peng, A. Nanayakkara, M. Challacombe, P.M.W. Gill, B. Johnson, W. Chen, M. W. Wong, C. Gonzalez, J.A. Pople, *GAUSSIAN 03*, Revision B.04; Gaussian, Inc., Pittsburgh, PA, 2003.
- [36] A.D. Becke, *J. Chem. Phys.* 98 (1993) 5648.
- [37] C. Lee, W. Yang, R.G. Par, *Phys. Rev. B* 37 (1988) 785.
- [38] G.A. Pateresson, M.A. Al-Laham, *J. Chem. Phys.* 94 (1991) 6081.
- [39] P.J. Hay, W.R. Wadt, *J. Chem. Phys.* 82 (1985) 299.
- [40] P.J. Hay, W.R. Wadt, *J. Chem. Phys.* 82 (1985) 270.
- [41] I. Fridovich, *Adv. Inorg. Biochem.* 1 (1979) 67.
- [42] C. Beauchamp, I. Fridovich, *Anal. Biochem.* 44 (1971) 276.
- [43] M. Lombard, C. Houée-Levin, D. Touati, M. Fontecave, V. Nivière, *Biochemistry* 40 (2001) 5032.
- [44] J. Seth, V. Palaniappan, D.F. Bocian, *Inorg. Chem.* 34 (1995) 2201.
- [45] W. Kaim, B. Schwederski, *Pure Appl. Chem.* 76 (2004) 351, and references cited therein.
- [46] D. Dolphin, T. Niem, R.H. Felton, I. Fujita, *J. Am. Chem. Soc.* 97 (1975) 5288.
- [47] R.M. Buchanan, J. Clafin, C.G. Pierpont, *Inorg. Chem.* 22 (1983) 2552.
- [48] H.-C. Chang, K. Mochizuki, S. Kitagawa, *Inorg. Chem.* 41 (2002) 4444.